Chemical Engineering Journal 94 (2003) 127–137

Chemical Engineering Journal

www.elsevier.com/locate/cej

Closed-form solution of abrasion and abrasion–dissolution kinetic models

Alessandra Adrover, Stefano Cerbelli, Massimiliano Giona*, Antonio Velardo

Dipartimento di Ingegneria Chimica, Università di Roma "La Sapienza", Via Eudossiana 18, 00184 Rome, Italy

Received 8 October 2002; accepted 11 January 2003

Abstract

We analyze and solve in closed form the population balance equations describing abrasion-dominated fragmentation processes and abrasion processes in the presence of chemical dissolution kinetics. The fragmentation model proposed takes into account that abrasion, at each breakup event, generates a manifold of smaller fragments characterized by a continuous distribution, with the constrain that the mass of fines produced at each breakup event is constant. The kinetic model for abrasion is applied to experimental data available in the literature.

Keywords: Abrasion; Dissolution; Population balances

1. Introduction

Grinding processes are characterized by several different fragmentation regimes [1]. A broad spectrum of size distributions results from grinding, depending upon energy input. Abrasion results from the application of low-intensity surface stresses, which ultimately leads to a bimodal particle size distribution corresponding to small fragments removed from the surface of larger fragments. Cleavage and fracture result from the application of more intense stresses. Cleavage produces fragments of size slightly smaller than the mother particles. Fracture produces a broad size distribution of child fragments.

In order to gain a quantitative description of fragmentation phenomena to be used for process design and optimization, two pieces of information are required: the fragmentation rate and the number and size of child particles resulting from the breakage of a mother particle, i.e. the fragmentation kernel. The fragmentation rate and kernel are typically determined directly from the experimental data, and several empirical fragmentation kernels have been obtained for specific process units and materials [2,3].

In addition to empirical kernels, some theoretical models based on physical arguments have been derived [4]. A general homogeneous model for multiple particle breakage attains the form

$$b(v, w) = \frac{\phi\lambda}{w}\left(\frac{v}{w}\right)^{\lambda-2} + (1-\phi)\frac{\kappa}{w}\left(\frac{v}{w}\right)^{\kappa-2}, \qquad (1)$$

where $b(v, w)$ is a number-based breakage distribution function, v and w the child and mother particle masses, and ϕ, κ and λ are three adjustable parameters.

Homogeneous kernels can hardly yield bimodal distributions as those resulting from abrasion. For abrasion-dominated fragmentation, Hansen and Ottino [5,6] proposed a simple impulsive fragmentation kernel describing the binary fragmentation of a mother particle of mass y into two particles of mass $\varepsilon \ll y$ and $y - \varepsilon$, respectively. Although the binary-abrasion model developed by Hansen and Ottino suffers from some inconsistencies, it is nonetheless a useful starting point for the development of more general models for a fragmentation process dominated by abrasion, leading to a continuous distribution of fines.

The aim of this article is to develop and solve in closed form an abrasion model which takes into account the fact that abrasion, at each breakup event, generates a manifold of fragments (fines) characterized by a continuous distribution.

The article is organized as follows. Section 2 reviews the abrasion models available in the literature, and discusses their limitations and drawbacks. Section 3 addresses in detail the abrasion model proposed. In the same section, the closed-form solution for the dynamics of the particle distribution function is derived. In Section 4, the model is applied to experimental data available in the literature, thus presenting a simple and effective approach for determining model parameters from the analysis of fragmentation data. Finally, Section 5 analyzes the influence of abrasion on the evolution of a kinetically controlled dissolution process. We develop a closed-form solution for the temporal evolution of the particle distribution function in the presence of both dissolution and abrasion.

* Corresponding author. Tel.: +39-06-44585609; fax: +39-06-44585451.
E-mail address: max@giona.ing.uniroma1.it (M. Giona).

1385-8947/03/$ – see front matter
doi:10.1016/S1385-8947(03)00024-X

Nomenclature

$a(x)$	fragmentation rate ($\tilde{a}(x) = a(x)/a(1)$)
$b(x; y)$	fragmentation kernel
$c(x, t)$	particle distribution function
$c^+(x, t)$	mother particle distribution
$c^-(x, t)$	fine particle distribution
$\hat{f}(s)$	Laplace transform of the generic function $f(\theta)$
$h(x)$	pdf of fines generated during abrasion
k_d	prefactor of the dissolution rate $r(x)$
k_f	prefactor of the fragmentation rate $a(x)$
$N(y)$	number of fragments generated by a particle of mass y
$r(x)$	dissolution rate due to chemical reactions ($\tilde{r}(x) = r(x)/a(1)$)
s	Laplace variable
t	time
x	mass
x_h	first-order moment of $h(x)$
x^*	threshold value for fines

Greek letters

β	localization exponent of $\omega(x)$
$\delta(x)$	Dirac's impulsive distribution
ε	mass of the fine particle in binary abrasion
θ	dimensionless time
κ	parameter of the homogeneous fragmentation kernel
λ	parameter of the homogeneous fragmentation kernel
μ	exponent of the fragmentation rate
ϕ	parameter of the homogeneous fragmentation kernel
$\omega(x)$	C^∞ compactly supported function defined by Eq. (21)

2. Literature models for abrasion

Let $c(x, t)$ be the distribution function for a mixture of solid particles so that $c(x, t)\,dx$ is the number of particles possessing mass between x and $x + dx$, at time t.

The population balance equation for linear fragmentation kinetics can be expressed by the integral equation:

$$\frac{\partial c(x,t)}{\partial t} = -a(x)c(x,t) + \int_x^\infty b(x;y)a(y)c(y,t)\,dy, \qquad (2)$$

where $a(x)$ is the fragmentation rate (s^{-1}), and $b(x; y)$ the fragmentation kernel representing the number of fragments of mass x resulting from the fragmentation of a particle of mass y.

Under the assumption that the fragmentation rate is proportional to the surface area, it follows that $a(x) = k_f x^\mu$, with $\mu = 2/3$.

Mass conservation implies that:

$$\int_0^y x\,b(x;y)\,dx = y, \qquad (3)$$

and the integral quantity

$$\int_0^y b(x;y)\,dx = N(y) \qquad (4)$$

yields the number $N(y)$ of fragments obtained from the breakup of a particle possessing mass y.

Eq. (3) stems from the fundamental constraint to be imposed on fragmentation models, i.e. mass conservation, which can be formally expressed as:

$$\int_0^\infty x\,c(x,t)\,dx = \text{constant}, \qquad \text{for all } t \geq 0. \qquad (5)$$

Abrasion is a particular fragmentation process in which small fragments are generated from the surface breakup of larger particles, yielding a typical bimodal distribution of mother particles and fines.

Hansen and Ottino [5,6] have analyzed this phenomenon, proposing a simple approximate model in the case of binary abrasion (i.e. $N(y) = 2$). The starting point is the assumption of an impulsive fragmentation kernel,

$$b(x;y) = \delta(x-(y-\varepsilon)) + \delta(x-\varepsilon), \qquad y \geq \varepsilon, \qquad (6)$$

where $\delta(x-x_c)$ is the Dirac's impulsive distribution centered at $x = x_c$. This kernel corresponds to the fragmentation of a generic particle of mass y into two fragments of mass $y-\varepsilon$ and ε, where $\varepsilon > 0$ is some constant value such that $\varepsilon \ll y$.

By substituting Eq. (6) into Eq. (2), one obtains the following functional equation for the particle distribution function:

$$\frac{\partial c(x,t)}{\partial t} = a(x+\varepsilon)c(x+\varepsilon,t) - a(x)c(x,t) + \delta(x-\varepsilon)\int_\varepsilon^\infty a(y)c(y,t)\,dy. \qquad (7)$$

The key simplification in the approach envisaged by Hansen and Ottino stems by approximating the difference of the two terms at the right-hand side of Eq. (7) by the corresponding derivative:

$$a(x+\varepsilon)c(x+\varepsilon,t) - a(x)c(x,t) \simeq \varepsilon\frac{\partial[a(x)c(x,t)]}{\partial x}, \qquad (8)$$

so that Eq. (7) becomes

$$\frac{\partial c(x,t)}{\partial t} = \varepsilon\left\{\frac{\partial[a(x)c(x,t)]}{\partial x} + \frac{\delta(x-\varepsilon)}{\varepsilon}\int_x^\infty a(y)c(y,t)\,dy\right\}. \qquad (9)$$

Eq. (9) is particularly appealing due to its simplicity. However, it needs some formal "make-up" to be fully consistent. Written as it is, Eq. (9) implies that the partial derivative term $\partial[a(x)c(x,t)]/\partial x$ acts for all values of x, and therefore also for $x < \varepsilon$. As a consequence of this, Eq. (9) does not

satisfy the fundamental requirement of mass conservation expressed by Eq. (5). To see this, it is sufficient to multiply each term in Eq. (9) by x and integrate over the whole mass range $[0, \infty)$, to get

$$\frac{\mathrm{d}}{\mathrm{d}t}\int_0^\infty x\,c(x,t)\,\mathrm{d}x = -\varepsilon\int_0^\infty a(x)c(x,t)\,\mathrm{d}x + \varepsilon\int_\varepsilon^\infty a(x)c(x,t)\,\mathrm{d}x = -\varepsilon\int_0^\varepsilon a(x)c(x,t)\,\mathrm{d}x. \quad (10)$$

If the support of the particle distribution function covers the region of fines, $x \in (0, \varepsilon)$—which is certainly true during an abrasion process—Eq. (10) indicates that the overall mass decreases in time.

Eq. (9) can be straightforwardly modified to overcome this inconsistency by assuming that the derivative term $\partial[a(x)c(x,t)]/\partial x$ acts only on particles possessing mass greater than ε, thus leading to the balance equation:

$$\frac{\partial c(x,t)}{\partial t} = \varepsilon\left\{\frac{\partial[a(x)c(x,t)]}{\partial x}\eta(x-\varepsilon) + \frac{\delta(x-\varepsilon)}{\varepsilon}\int_x^\infty a(y)c(y,t)\,\mathrm{d}y\right\}, \quad (11)$$

where $\eta(x - x_\mathrm{c})$ is the Heaviside step function:

$$\eta(x-x_\mathrm{c}) = \begin{cases} 0 & x < x_\mathrm{c} \\ 1 & x > x_\mathrm{c}. \end{cases} \quad (12)$$

However, even this modification leads to an abrasion model that is inconsistent from the mass conservation point of view, since from Eq. (11) it follows that:

$$\frac{\mathrm{d}}{\mathrm{d}t}\int_0^\infty x\,c(x,t)\,\mathrm{d}x = -\varepsilon^2 a(\varepsilon)c(\varepsilon,t). \quad (13)$$

This result is a consequence of the discontinuity occurring at $x = \varepsilon$.

In point of fact, all these shortcomings can be overcome by a slight reformulation of Eq. (8). By assuming that $a(x) = 0$ for $x < \varepsilon$, i.e. that no fragmentation occurs for particles possessing mass less than the threshold value ε, the approximation (8) can be modified as follows:

$$a(x+\varepsilon)c(x+\varepsilon,t) - a(x)c(x,t) \simeq \varepsilon\frac{\partial[a(x)c(x,t)]}{\partial x}\eta(x-\varepsilon) + \varepsilon a(\varepsilon)c(\varepsilon,t)\delta(x-\varepsilon). \quad (14)$$

The first term at the right-end side accounts for the approximation for $x > \varepsilon$. The second, impulsive term derives from the discontinuity at $x = \varepsilon$.

By substituting Eq. (14) into Eq. (7), the following equation is obtained:

$$\frac{\partial c(x,t)}{\partial t} = \varepsilon\left\{\frac{\partial[a(x)c(x,t)]}{\partial x}\eta(x-\varepsilon) + \frac{\delta(x-\varepsilon)}{\varepsilon} \times \left(\int_x^\infty a(y)c(y,t)\,\mathrm{d}y + \varepsilon a(x)c(x,t)\right)\right\}, \quad (15)$$

which yields a consistent approximation for binary fragmentation, satisfying mass conservation Eq. (5) for any initial choice of the particle distribution function.

Although Eq. (14) may appear rather artificial, it follows straightforwardly from the assumption that the fragmentation rate vanishes for $x < \varepsilon$, by enforcing the same level of approximation for the derivative envisaged by Hansen and Ottino. Since by hypothesis $a(x) = 0$ for $x < \varepsilon$, it results $a(x) = a(x)\eta(x-\varepsilon)$. Therefore, the left-hand side of Eq. (8) can be expressed as:

$$a(x+\varepsilon)\eta(x)c(x+\varepsilon) - a(x)\eta(x-\varepsilon)c(x,t) \simeq \varepsilon\frac{\partial[a(x)\eta(x-\varepsilon)c(x,t)]}{\partial x} = \varepsilon\frac{\partial[a(x)c(x,t)]}{\partial x}\eta(x-\varepsilon) + \varepsilon a(x)c(x,t)\delta(x-\varepsilon) \quad (16)$$

which is Eq. (14) since

$$a(x)c(x,t)\delta(x-\varepsilon) = a(\varepsilon)c(\varepsilon,t)\delta(x-\varepsilon).$$

To conclude this section, let us briefly address the physical meaning of the basic assumption on the fragmentation rate $a(x)$. Abrasion is essentially associated with the superficial breakup of large particles due to collisions and mechanical friction. It is fairly reasonable to assume that this phenomenon involves exclusively larger particles and not fines, so that $a(x) = 0$ for $x < \varepsilon$. in point of fact this assumption can be viewed as one of the main qualitative differences between the modelling of abrasion compared to other fragmentation processes, which can be described by means of homogeneous kernels, such as Eq. (1) expressing a fragmentation cascade at all the length-scales.

3. Generalized abrasion model

Eq. (15) can be taken as a useful starting point for the development of a more general and consistent model for abrasive fragmentation. The need for a model generalization stems from its application to experimental (laboratory, process) data. In practical applications, Eq. (15) suffers of two main shortcomings:

- the fragmentation process described is binary, while abrasion is intrinsically characterized by the simultaneous generation of a manifold of smaller fragments;
- the fragmentation kernel Eq. (6) generates fines all of the same mass ε, whereas a continuous spectrum of fines is observed in practice.

In the following two subsections, we develop and solve in closed form a simple model of abrasion, accounting for the two issues mentioned above, which may be referred to as the generalized abrasion model (GAM).

3.1. Model formulation

Without loss of generality we assume that x represents a dimensionless mass, so that $x = 1$ is the dimensionless mass of the largest particle in the initial particle mixture.

The model can be derived from the following assumptions:

1. There exists a threshold value $x^* < 1$ of x, such that no fragmentation occurs for $x < x^*$. This implies that
$$a(x) = 0, \qquad x < x^*. \tag{17}$$
2. Each mother particle of mass $y > x^*$ breaks up into $(N + 1)$ fragments: the eroded mother particle of mass $y - x^*$ and a swarm of N fine fragments of masses $\{x_i\}_{i=1}^{N}$, with the constraint
$$\sum_{i=1}^{N} x_i = x^*, \tag{18}$$
as depicted in Fig. 1. Eq. (18) expresses the elementary fact that the mass of fines produced at each breakup event is constant.
3. The mass of the abraded fragments is distributed over the interval $[0, x^*]$, according to a given probability density function $h(x)$.

These model assumptions, (specifically, assumptions 2 and 3), imply that the fragmentation kernel can be expressed as:

$$b(x; y) = \delta(x - (y - x^*)) + N\,h(x), \tag{19}$$

where $h(x)$ is a compactly supported function defined on $[0, x^*]$ attaining non-negative values. The function $h(x)$ controls the shape of the distribution of fines generated during abrasion.

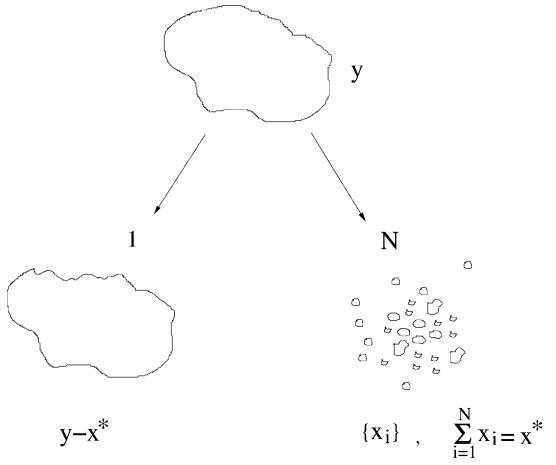

Fig. 1. Schematic representation of the generalized abrasion process.

The compact nature of the support over which $h(x)$ is defined can be ensured by assuming that:

$$h(x) = \tilde{h}(x)\omega(x), \tag{20}$$

where $\tilde{h}(x)$ is a generic non-negative continuous function, and $\omega(x)$ is a C^∞ compactly supported function defined by:

$$\omega(x) = \begin{cases} \exp\left[\beta + \dfrac{\beta(x^*)^2}{(2x - x^*)^2 - (x^*)^2}\right], & \text{for } |x - x^*/2| < x^*/2, \\ 0, & \text{elsewhere,} \end{cases} \tag{21}$$

The function $\omega(x)$ depends on the parameter β, which modulates its shape around $x = x^*$. Eq. (21) is the expression for a classical compactly supported function, widely used in the theory of distribution as regularization kernel [7]. From Eqs. (20) and (21) it follows that $h(0) = h(x^*) = 0$.

The function $h(x)$ should satisfy some constraints deriving from model assumptions:

1. The $(N + 1)$-ary nature of the process implies
$$\int_0^y b(x; y)\,\mathrm{d}x = N + 1 \rightarrow \int_0^{x^*} h(x)\,\mathrm{d}x = 1, \tag{22}$$
that is, $h(x)$ is a normalized probability density function on $[0, x^*]$.
2. Mass conservation Eq. (3) implies
$$x_h = \int_0^{x^*} x\,h(x)\,\mathrm{d}x = \frac{x^*}{N}, \tag{23}$$
that is the first-order moment x_h of the distribution $h(x)$ equals the ratio between the threshold mass x^* and the number of fine particles N.

By substituting Eq. (19) for the abrasion kernel into the linear fragmentation equation Eq. (2), one obtains the following balance equation:

$$\frac{\partial c(x,t)}{\partial t} = a(x + x^*)c(x + x^*, t) - a(x)c(x, t) + N\,h(x)\int_{x^*}^{\infty} a(y)c(y, t)\,\mathrm{d}y. \tag{24}$$

The difference $[a(x + x^*)c(x + x^*, t) - a(x)c(x, t)]$ can be approximated, as discussed in Section 2, as follows:

$$a(x + x^*)c(x + x^*, t) - a(x)c(x, t) \simeq x^*\frac{\partial[a(x)c(x,t)]}{\partial x}\eta(x - x^*) + x^*\,a(x^*)c(x^*, t)\delta(x - x^*), \tag{25}$$

thus introducing an impulsive contribution at $x = x^*$. Abrasion kinetics yields a continuous distribution of fines possesing an invariant shape, which in the model is proportional to the probability density function $h(x)$. This leads to a physically reasonable approximation for Eq. (25), consisting of

replacing the impulsive contribution with a smooth term proportional to $h(x)$, which corresponds to the redistribution of fines according to the invariant pdf $h(x)$

$$x^* a(x^*)c(x^*,t)\delta(x-x^*) \rightarrow b\, a(x^*)c(x^*,t)h(x). \tag{26}$$

The parameter b is a constant, the value of which follows from mass conservation.

By enforcing that the two terms appearing in Eq. (26) possess the same first-order moment, the constant b can be expressed as:

$$b = \frac{(x^*)^2}{x_h}. \tag{27}$$

By substituting Eqs. (25)–(27) into Eq. (24), the following kinetic model for abrasion is obtained:

$$\begin{aligned}\frac{\partial c(x,t)}{\partial t} &= x^* \frac{\partial[a(x)c(x,t)]}{\partial x}\eta(x-x^*) \\ &\quad + h(x)\left[N\int_{x^*}^{\infty} a(y)c(y,t)\,\mathrm{d}y \right. \\ &\quad \left. + \frac{(x^*)^2}{x_h}a(x^*)c(x^*,t)\right].\end{aligned} \tag{28}$$

It is straightforward to check that Eq. (28) satisfies mass conservation, i.e. Eq. (5).

By introducing the dimensionless time $\theta = tx^* a(1)$ and the dimensionless fragmentation rate $\tilde{a}(x) = a(x)/a(1)$ (under the hypothesis that $a(1) \neq 0$), Eq. (28) attains the form:

$$\begin{aligned}\frac{\partial c(x,\theta)}{\partial \theta} &= \frac{\partial[\tilde{a}(x)c(x,\theta)]}{\partial x}\eta(x-x^*) \\ &\quad + \frac{h(x)}{x_h}\left[\int_{x^*}^{\infty} \tilde{a}(y)c(y,\theta)\,\mathrm{d}y \right. \\ &\quad \left. + x^*\tilde{a}(x^*)c(x^*,\theta)\right].\end{aligned} \tag{29}$$

It is convenient to subdivide the particle population $c(x,\theta)$ into two classes, corresponding to the natural discrimination typical of abrasion processes, namely original mother particles, characterized by a distribution $c^+(x,\theta)$, and fines, characterized by a distribution $c^-(x,\theta)$:

$$\begin{aligned}c^+(x,\theta) &= \begin{cases} 0, & x < x^* \\ c(x,t), & x \geq x^* \end{cases}, \\ c^-(x,\theta) &= \begin{cases} c(x,t), & x < x^* \\ 0, & x \geq x^* \end{cases},\end{aligned} \tag{30}$$

By enforcing this subdivision, the model equations attain the form:

$$\frac{\partial c^+(x,\theta)}{\partial \theta} = \frac{\partial[\tilde{a}(x)\,c^+(x,\theta)]}{\partial x}, \qquad x > x^*, \tag{31}$$

$$\begin{aligned}\frac{\partial c^-(x,\theta)}{\partial \theta} &= \frac{h(x)}{x_h}\left[\int_{x^*}^{\infty} \tilde{a}(y)\,c^+(y,\theta)\,\mathrm{d}y \right. \\ &\quad \left. + x^*\tilde{a}(x^*)c^+(x^*,\theta)\right], \qquad x < x^*.\end{aligned} \tag{32}$$

The solution of Eq. (29)—or equivalently of Eqs. (31) and (32)—is discontinuous at $x = x^*$, yet the cumulative mass fraction $M(x,\theta)$

$$M(x,\theta) = \frac{\int_0^x yc(y,\theta)\,\mathrm{d}y}{\int_0^{\infty} yc(y,\theta)\,\mathrm{d}y} \tag{33}$$

is continuous with respect to x.

The shape of the function $h(x)$ is in principle arbitrary, except that it should fulfill the constraints Eqs. (22) and (23). In the particular case of a binary fragmentation, from Eqs. (22) and (23) it follows that

$$\int_0^{x^*} h(x)\,\mathrm{d}x = 1, \qquad \int_0^{x^*} x\,h(x)\,\mathrm{d}x = x^*. \tag{34}$$

and the only function satisfying these conditions is a Dirac's delta distribution, $h(x) = \delta(x-x^*)$. In this case, the model reduces to Eq. (15) discussed in Section 2.

The model proposed puts on a formal basis the qualitative approach envisaged by Hansen and Ottino [5,6], who solve a binary fragmentation model, thus obtaining a Dirac's delta distribution for fines, and then replace, on an intuitive basis, the singular distribution of fines with a smooth distribution function $h(x)$, without providing any expression for the fragmentation kernel and without discussing the basic constraints on the distribution function $h(x)$.

3.2. Closed-form solution

The Generalized Abrasion Model (GAM) developed in Section 3.1 admits a closed-form solution, for any choice of the fragmentation rate $a(x)$ and of the fine pdf $h(x)$. The simplest way to obtain it is to make use of Laplace transforms. Let $\hat{c}^+(x,s)$ be the Laplace transform of $c^+(x,\theta)$. In the Laplace domain, Eq. (31) becomes:

$$s\,\hat{c}^+(x,s) - c_0(x) = \frac{\mathrm{d}[\tilde{a}(x)\hat{c}^+(x,s)]}{\mathrm{d}x}, \tag{35}$$

where $c_0(x) = c(x,\theta)|_{\theta=0}$ is the initial particle distribution. Specifically, we assume that $c_0(x) = 0$ for $x < x^*$, i.e. no fines are initially present in the mixture. By defining $\hat{g}(x,s) = \tilde{a}(x)\hat{c}^+(x,s)$, Eq. (35) becomes:

$$\frac{\mathrm{d}\hat{g}(x,s)}{\mathrm{d}x} = \frac{s\,\hat{g}(x,s)}{\tilde{a}(x)} - c_0(x). \tag{36}$$

By introducing the auxiliary function $H(x)$:

$$H(x) = \int_{x^*}^{x} \frac{\mathrm{d}y}{\tilde{a}(y)}, \tag{37}$$

the solution of Eq. (36) is given by

$$\begin{aligned}\hat{g}(x,s) &= C\exp[s(H(x)-H(u))] \\ &\quad - \int_u^x c_0(y)\exp[s(H(x)-H(y))]\,\mathrm{d}y,\end{aligned} \tag{38}$$

where C is a constant and u is an arbitrary initial value. By enforcing the regularity for $x \rightarrow \infty$, i.e. by letting $u = \infty$,

it follows that $C = 0$ so that:

$$\hat{g}(x,s) = \int_x^\infty c_0(y)\exp[s(H(x) - H(y))]\,\mathrm{d}y. \tag{39}$$

The inverse Laplace transform of $\hat{g}(x,s)$ is given by

$$g(x,\theta) = \int_x^\infty c_0(y)\,\delta(\theta + H(x) - H(y))\,\mathrm{d}y, \tag{40}$$

or equivalently

$$g(x,\theta) = \tilde{a}(w(x,\theta))\,c_0(w(x,\theta)), \tag{41}$$

where

$$w(x,\theta) = H^{-1}(H(x) + \theta). \tag{42}$$

Correspondingly, the distribution function $c^+(x,\theta)$ for mother particles attains the form:

$$c^+(x,\theta) = \frac{\tilde{a}(w(x,\theta))\,c_0(w(x,\theta))}{\tilde{a}(x)}. \tag{43}$$

Given $c^+(x,\theta)$, the distribution functions for fines $c^-(x,\theta)$ can be obtained from Eq. (32) by quadratures, i.e.

$$c^-(x,\theta) = \frac{h(x)}{x_h}\int_0^\theta \left[\int_{x^*}^\infty \tilde{a}(w(y,\theta'))\,c_0(w(y,\theta'))\,\mathrm{d}y + x^*\,\tilde{a}(w(x^*,\theta'))\,c_0(w(x^*,\theta'))\right]\mathrm{d}\theta'. \tag{44}$$

In the particular case, $\tilde{a}(x)$ admits a power-law expression $\tilde{a}(x) = x^\mu$, such as for fragmentation rates proportional to the particle surface area, it follows that:

$$H^{-1}(H(x) + \theta) = w(x,\theta) = \left[x^{1-\mu} + \theta(1-\mu)\right]^{1/(1-\mu)}. \tag{45}$$

To provide an example, let us consider a log–normal shape for $\tilde{h}(x)$:

$$\tilde{h}(x) = \frac{A}{\sigma\sqrt{2\pi}x}\exp\left[-\frac{(\ln x - \eta)^2}{2\sigma^2}\right], \tag{46}$$

where σ and η are two parameters controlling the variance and the mean of the distribution. The prefactor A is a normalization constant, such that the integral of the function $h(x) = \tilde{h}(x)\omega(x)$ over the interval $[0, x^*]$ equals 1. For the localization exponent β characterizing shape of the compactly supported function $\omega(x)$, the value $\beta = 0.01$ has been chosen. The value of the dimensionless threshold mass is set to $x^* = 0.7$.

The shape of the distribution $h(x)$ controls the number N of fine fragments generated at each erosion event. From Eq. (23), it follows that N is the ratio between the threshold mass x^* and the first-order moment x_h of the distribution $h(x)$. Fig. 2 shows the behavior of N as a function of the parameter η for two different values of σ (curve a, $\sigma = 0.1$; curve b, $\sigma = 1.0$). For a given $h(x)$, the value of N is uniquely specified. The results depicted in this figure can be applied in a reverse way: suppose we fix the value of σ and N. From the curves of Fig. 2 it is possible to read the proper value of η giving rise to a prescribed fragmentation process.

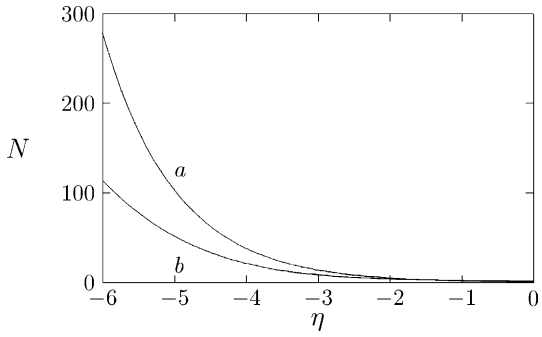

Fig. 2. N vs. η for a log–normal $\tilde{h}(x)$. Curves a and b refer, respectively, to $\sigma = 0.1$ and 1.0.

Fig. 3A–D show the behavior of the function $x\,c(x,\theta)$ for several time instants, starting from the same initial distribution, for two different choices of the parameters σ and η, corresponding to the same value of $N = 50$. The initial distribution $c_0(x)$, has been assumed equal to the product of $\omega(x)$—centered at $x = 0.5$, i.e. obtained by replacing x^* with 0.5 in Eq. (21)—times a log–normal distribution with $\eta = 2$ and $\sigma = 0.2$.

In order to highlight the behavior of the distributions of mother particles and fines, the behavior below and above x^* is depicted on two separate figures. It can be observed that,

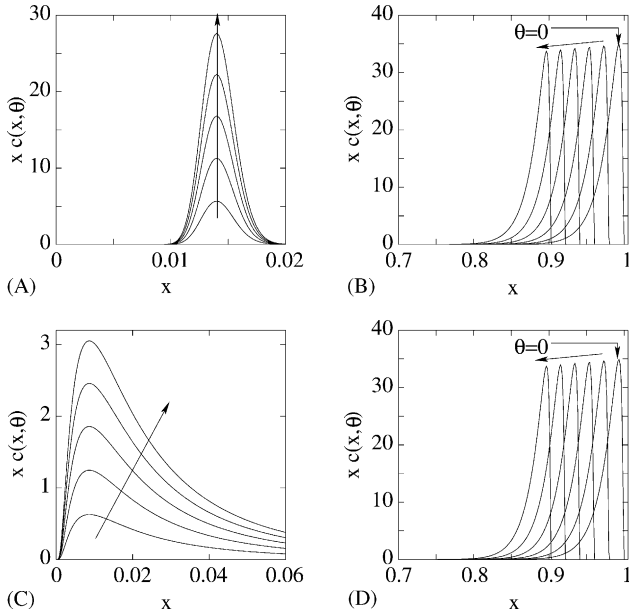

Fig. 3. $x\,c(x,\theta)$ vs. x at several different time instants, $\theta = 0, 0.02, 0.04, 0.06, 0.08, 0.1$ for the same initial log–normal distribution and log–normal behavior of $\tilde{h}(x)$, and for two different values of σ. Both simulations refers to the same number of fragments $N = 50$ ($x^* = 0.7$). (A) $\sigma = 0.1$, $\eta = -4.3$; (B) $\sigma = 1$, $\eta = -4.9$. Parts A and C show the distribution of fines and parts B and D show the distribution of mother particles.

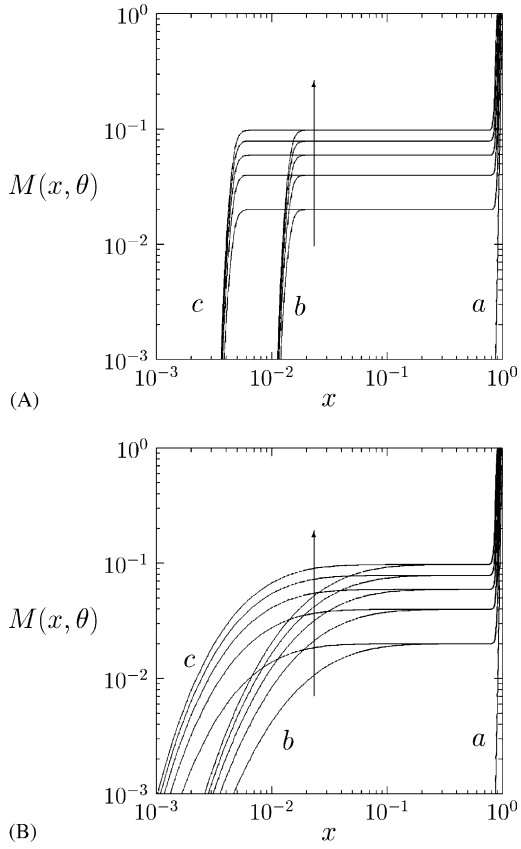

Fig. 4. Log–log plot of cumulative mass fraction $M(x,\theta)$ vs. x at several different time instants, $\theta = 0, 0.02, 0.04, 0.06, 0.08, 0.1$, for the same initial log–normal distribution (curve a) and log–normal behavior of $\tilde{h}(x)$, and for two different number of fragments $N = 50, 150$ ($x^* = 0.7$). (A) $\sigma = 0.1$, $N = 50$ ($\eta = -4.3$, bundle of curve b), and $N = 150$ ($\eta = -5.4$, bundle of curve c). (B) $\sigma = 1$, $N = 50$ ($\eta = -4.9$, bundle of curve b), and $N = 150$ ($\eta = -6.4$, bundle of curve c).

in both cases, the dynamics of mother particle distribution ($x > x^*$) is identical while the functional form of $h(x)$, for fixed N, modifies the shape of the resulting distribution of fines.

The effects of the shape of $h(x)$ on the cumulative mass fraction $M(x,\theta)$ are depicted in Fig. 4A and B for two different values of σ and two different values of N. As expected, higher values of σ generate much broader distributions of fines (compare Fig. 4B for $\sigma = 1$ with Fig. 4A for $\sigma = 0.1$).

The formal structure of the model is suitable to approach parameter estimation in a simple and effective way starting from experimental data of batch fragmentation. This is the topic of the next section.

4. Analysis of batch fragmentation data

The GAM developed in Section 3 describes fragmentation kinetics due to abrasion in which a mother particle breaks up into N fine fragments, giving rise to a continuous distribution of fines. Moreover, the shape of the distribution of fines is invariant and proportional to $h(x)$, since for any $\theta > 0$:

$$\frac{c^-(x,\theta) - c^-(x,0)}{\int_0^{x^*}[c^-(y,\theta) - c^-(y,0)]\,\mathrm{d}y} = h(x), \tag{47}$$

Starting from this observation it is possible to develop a simple and consistent approach for the analysis of fragmentation experiments, which yields model parameters and functions in a straightforward way.

Under the assumption that the fragmentation rate is controlled by the particle surface area, the parameters to be determined are: (a) the threshold value x^*, separating mother particles and fines; (b) the shape of the function $h(x)$, corresponding to the distribution of fines generated during abrasion; (c) the time constant $a(1)$, corresponding to the fragmentation rate for particles of dimensionless unit mass.

In order to exemplify data analysis resulting from the application of the GAM, we consider the breakage of potassium sulfate crystals in an agitated vessel, which displays a typical abrasion behavior. The data are taken from [11], and the reader is referred to this article for further details on the experimental set-up. Fig. 5 shows the cumulative mass distributions at different time instants $t = 0.5, 1, 4, 6, 10$ h.

The initial distribution, (first curve from the bottom in Fig. 5, corresponding to a time instant $t = 0.5$ h), contains a fraction of fine particles. The values of x^* can be estimated from the point at which the slope of $M(x,\theta)$ exhibits a sudden change, (in the present case $x^* = 0.3$).

The shape of $h(x)$ can be determined directly from the experimental data. If experimental data correspond to an abrasion process, we expect that the difference $c^-(x,t) - c^-(x,t_0)$, for $t > t_0$, attains an invariant shape modulo a multiplicative constant,

$$c^-(x,t) - c^-(x,t_0) = B\,h(x), \qquad x < x^*, \tag{48}$$

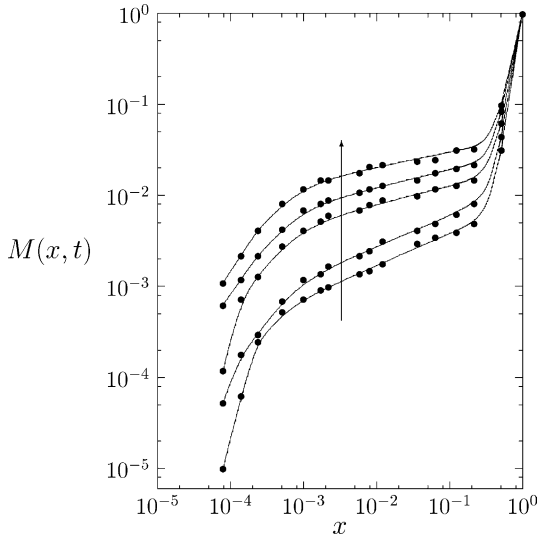

Fig. 5. Log–log plot of the experimental cumulative mass fraction $M(x,t)$ vs. x from [11], at several increasing time instant, $t = 0.5, 1, 4, 6, 10$ [h].

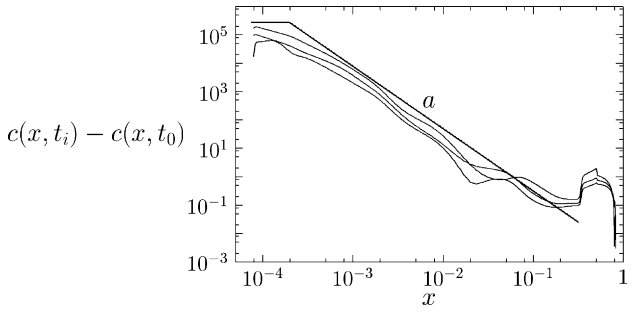

Fig. 6. Log–log plot of $c(x,t_i)-c(x,t_0)$ vs. x ($i=2,3,4$) evaluated from the interpolation of experimental data by [11] depicted in Fig. 5 ($t_0=0.5$ h; $t_2=4$ h; $t_3=6$ h; $t_4=10$ h). Line a corresponds to the approximated behavior of $\tilde{h}(x)$. Eq. (49) modulo a normalization constant.

where B is some positive constant. The reference profile $c^-(x,t_0)$ could be in principle arbitrary, and the most natural choice is to take the initial profile (in this case $t_0=0.5$ h).

Fig. 6 shows the behavior of the difference function $c^-(x,t)-c^-(x,t_0)$ at $t=4,6,10$ h, obtained from the experimental data depicted in Fig. 5. The experimental difference functions have been obtained from the cumulative mass fraction distributions depicted in Fig. 5, upon intepolation, by taking the derivate with respect to x and by multiplying the result by $1/x$. As can be observed from Fig. 6, the basic model assumption Eq. (48) is satisfied, within the range of experimental error. Indeed, for $x<x^*$ ($x^*=0.3$), all data are proportional to a single master curve (curve a in Fig. 6), which can be expressed analytically as follows

$$\tilde{h}(x)=\begin{cases} Ax_1^{-b}, & x\le x_1 \\ Ax^{-b}, & x>x_1 \end{cases} \tag{49}$$

where $x_1=2\times10^{-4}$, $b=2.2$ and A is the normalization constant such that the integral of $\tilde{h}(x)\omega(x)$ equals 1.

Therefore, the value and the expression of the main quantities entering the fragmentation model follow immediately from the direct analysis of the experimental data.

As a by-product of the direct identification of the distribution function $h(x)$, it follows the value of N, i.e. the number of fragments generated by a single breakup event, which in the present case yields $N\simeq600$.

For a complete identification of the model we are left with estimating the kinetic coefficient $k_f=a(1)$, i.e. the prefator entering the expression for the fragmentation rate and controlling the time-scale of the dynamics of the process. The estimate for the prefactor k_f can be achived with standard optimization tools and yields, in the present case, $k_f=0.883\times10^{-4}\,\mathrm{h}^{-1}$.

The comparison of model predictions and experimental results is depicted in Fig. 7. As can be observed, the agreement is satisfactory (small deviations from experimental data can be observed at $x\simeq0.5$ at large time-scales ($t=6$ and 10 h)) thus showing that the model proposed is able to capture the essence of a fragmentation process controlled by abrasion.

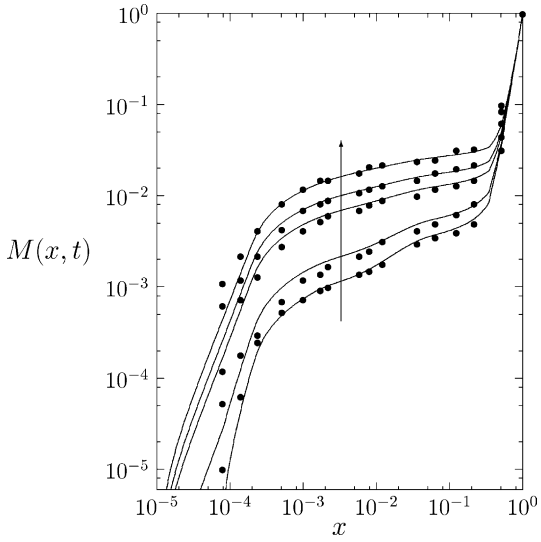

Fig. 7. Log–log plot of the mass fraction $M(x,t)$ vs. x obtained by applying the GAM (continuous line) compared with experimental data (dots) by [11] at the same time instants.

5. Fragmentation dissolution processes

Fragmentation processes may deeply influence the outcome of a chemical dissolution process, as recently observed by Tsai and Huang [8] who analyzed the interaction between abrasion and dissolution of aluminium in a phosphoric acid solution. General scaling results on the interplay between dissolution and fragmentation has been obtained by Edwards et al. [9] and Cai et al. [10].

In this section, we analyse the influence of abrasion phenomena on dissolution kinetics, within the framework of the GAM developed earlier.

5.1. Model formulation

The balance equation for a dissolution–abrasion process can be straightforwardly obtained as a generalization of Eq. (29), by including the effects of dissolution kinetics, which contributes as a first-order derivative term:

$$\frac{\partial c(x,\theta)}{\partial\theta}=\frac{\partial[\tilde{a}(x)c(x,\theta)]}{\partial x}\eta(x-x^*)+\frac{\partial[\tilde{r}(x)c(x,\theta)]}{\partial x}+\frac{h(x)}{x_h}\left[\int_{x^*}^{\infty}\tilde{a}(y)c(y,\theta)\,\mathrm{d}y+x^*\,\tilde{a}(x^*)c(x^*,\theta)\right] \tag{50}$$

where $\tilde{r}(x)=r(x)/a(1)$ is the dimensionless rate of mass loss due to chemical dissolution. In the case of kinetic control of the dissolution process, the dissolution rate $r(x)$ is proportional to the wetted surface, and the further assumption that the particles are spherical yields $r(x)=k_dx^\mu$, so that $\tilde{r}(x)=(k_d/k_f)x^\mu$.

By enforcing the natural decomposition into mother particles and fines, the kinetic model Eq. (50) can be

reformulated as follows:

$$\frac{\partial c^+(x,\theta)}{\partial \theta} = \frac{\partial[\tilde{q}(x)\, c^+(x,\theta)]}{\partial x}, \qquad x \geq x^*, \tag{51}$$

$$\frac{\partial c^-(x,\theta)}{\partial \theta} = \frac{\partial[\tilde{r}(x)\, c^-(x,\theta)]}{\partial x} + \frac{h(x)}{x_h} \times \left[\int_{x^*}^{\infty} \tilde{a}(y)\, c^+(y,\theta)\, \mathrm{d}y + x^*\, \tilde{a}(x^*) c^+(x^*,\theta)\right], \quad x < x^*, \tag{52}$$

where

$$\tilde{q}(x) = \tilde{a}(x) + \tilde{r}(x). \tag{53}$$

5.2. Closed-form solution

A closed-form solution for the model of fragmentation–dissolution developed in Section 5.1 follows directly from the analysis developed in the case of pure fragmentation. By introducing the auxiliary function:

$$K(x) = \int_{x^*}^{x} \frac{\mathrm{d}y}{\tilde{q}(y)}, \tag{54}$$

the function $c^+(x,\theta)$ attains the form

$$c^+(x,\theta) = \frac{\tilde{q}(z(x,\theta))\, c_0(z(x,\theta))}{\tilde{q}(x)}, \tag{55}$$

where:

$$z(x,\theta) = K^{-1}(K(x) + \theta). \tag{56}$$

In the particular case of kinetic control, and fragmentation rates proportional to the external surface,

$$\tilde{q}(x) = \tilde{a}(x) + \tilde{r}(x) = (1+\alpha)x^{\mu}, \qquad \alpha = \frac{k_\mathrm{d}}{k_\mathrm{f}}, \tag{57}$$

and the auxiliary function $z(x,\theta)$ attains the form:

$$z(x,\theta) = \left[x^{1-\mu} + \theta(1-\mu)\,(1+\alpha)\right]^{1/(1-\mu)}. \tag{58}$$

Therefore, under kinetic control of the dissolution process, the distribution of mother particles is the same as in the case of a pure abrasion process, but shifted in time by a factor $(1+\alpha)$.

In a similar way, a closed-form expression for the distribution of fines $c^-(x,\theta)$ can be obtained by making use of Laplace transfoms. Let us define the Laplace transforms:

$$\hat{f}(x,s) = \mathcal{L}\left[\tilde{r}(x)\, c^-(x,\theta)\right], \tag{59}$$

$$\hat{\gamma}(x^*,s) = \mathcal{L}\left[\frac{1}{x_h}\int_{x^*}^{\infty} \tilde{a}(y)\, c^+(y,\theta)\, \mathrm{d}y + x^*\, \tilde{a}(x^*)\, c^+(x^*,\theta)\right], \tag{60}$$

where $\mathcal{L}[\cdot]$ indicates Laplace transform. In the Laplace domain, Eq. (52) attains the form:

$$\frac{\partial \hat{f}(s,x)}{\partial x} = s\,\frac{\hat{f}(s,x)}{\tilde{r}(x)} - c_0(x) - h(x)\,\hat{\gamma}(x^*,s). \tag{61}$$

By introducing the auxiliary function:

$$N(x) = \int_0^x \frac{\mathrm{d}\xi}{\tilde{r}(\xi)}, \tag{62}$$

the solution of Eq. (61) can be expressed as:

$$\hat{f}(x,s) = \hat{f}(x^*,s)\,\mathrm{e}^{s[N(x)-N(x^*)]} - \int_{x^*}^{x} [c_0(y) + h(y)\,\gamma(x^*,s)]\,\mathrm{e}^{-s[N(y)-N(x)]}\,\mathrm{d}y, \tag{63}$$

which, in the time domain, becomes:

$$f(x,\theta) = f(x^*,\theta-\varphi_1(x))\,\eta(\theta-\varphi_1(x)) + c_0(p(x,\theta))\,\tilde{r}(p(x,\theta)) + \int_x^{x^*} h(y)\gamma(x^*,\theta-\varphi_2(x,y)) \times \eta(\theta-\varphi_2(x,y))\,\mathrm{d}y, \tag{64}$$

where,

$$p(x,\theta) = N^{-1}(N(x)+\theta), \tag{65}$$

$$\varphi_1(x) = N(x^*) - N(x), \tag{66}$$

$$\varphi_2(x,y) = N(y) - N(x). \tag{67}$$

By enforcing the continuity of the flux of particles at $x = x^*$,

$$f(x^*,\theta) = c^-(x^*,\theta)\tilde{r}(x^*) = c^+(x^*,\theta)\,\tilde{q}(x^*), \tag{68}$$

we obtain the closed-form expression for the distribution of fines:

$$c^-(x,\theta) = \frac{\tilde{q}(x^*,\theta-\varphi_1(x))}{\tilde{r}(x)}\, c^+(x^*,\theta-\varphi_1(x))\,\eta(\theta-\varphi_1(x)) + \frac{\tilde{r}(p(x,\theta))}{\tilde{r}(x)}\, c_0(p(x,\theta)) + \frac{1}{\tilde{r}(x)}\int_x^{x^*} h(y)\gamma(x^*,\theta-\varphi_2(x,y)) \times \eta(\theta-\varphi_2(x,y))\,\mathrm{d}y \tag{69}$$

where $c^+(x,\theta)$ is given by Eq. (55).

To give a numerical example, we analyze the influence of kinetically controlled dissolution on the abrasion processes depicted in Fig. 3A–D. The ratio $\alpha = k_\mathrm{d}/k_\mathrm{f}$ is set to 2. Fig. 8A–D show the behavior of $x\,c(x,\theta)$ at different time instants for $\sigma = 0.1$ and $\sigma = 1$, respectively. Fig. 9A and B show the corresponding behavior of the cumulative mass fraction $M(x,\theta)$.

As expected, the distribution of mother particles at time θ is the same as in the absence of dissolution at time $\theta\,(1+\alpha)$.

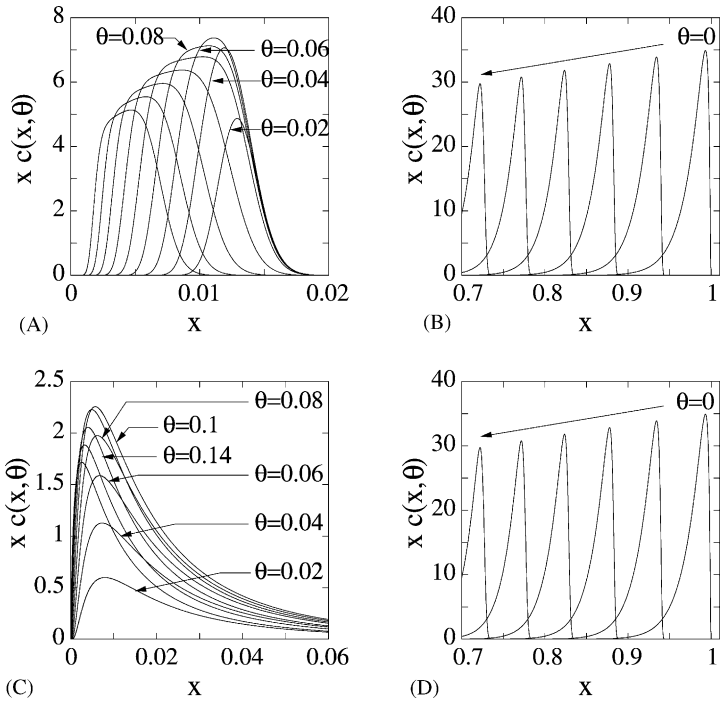

Fig. 8. $x\,c(x,\theta)$ vs. x for a dissolution–abrasion process ($\alpha = 2$), at different time instants $\theta = n\,\Delta\theta$, $n = 0, \ldots, 10$, $\Delta\theta = 0.02$ for the same initial log–normal distribution and log–normal behavior of $\tilde{h}(x)$. The distributions of mother particles and fines are reported in two different figures. (A and B) $x^* = 0.7$, $\sigma = 0.1$, $\eta = -4.3$ ($N \simeq 50$). (C and D) $x^* = 0.7$, $\sigma = 1$, $\eta = -4.9$ ($N = 50$).

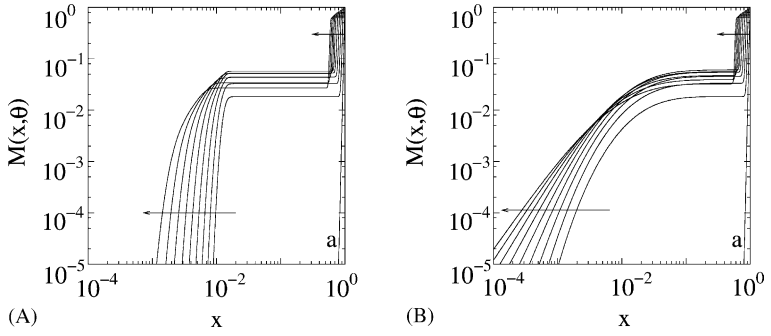

Fig. 9. Log–log plot of the cumulative mass fraction $M(x,\theta)$ vs. x for a dissolution–abrasion process ($\alpha = 2$), at different time instants $\theta = n\Delta\theta$, $n = 0, \ldots, 10$, $\Delta\theta = 0.02$, for the same initial log–normal distribution (curve a) and log–normal behavior of $\tilde{h}(x)$. (A) $x^* = 0.7$, $\sigma = 0.1$, $\eta = -4.3$ ($N \simeq 50$). (B) $x^* = 0.7$, $\sigma = 1$, $\eta = -4.9$ ($N = 50$).

Regarding the distribution of fines, we observe that the presence of dissolution induces the distribution to move in time towards lower values of x, and generates a progressive broadening. Moreover, the value at which the distribution attains its local maximum exhibits a non-monotonic behavior in time. Specifically, this value grows in time at short time scales, when the abrasion process starts to generate fines. Subsequently, the interplay between dissolution and abrasion induces a progressive decrease in time of the maximum abscissa towards zero, as can also be observed from the analysis of the temporal evolution of the cumulative mass fraction $M(x,\theta)$.

6. Conclusions

In this paper, we have proposed a simple abrasion model, referred to as GAM that by generalizing the approach originally developed by Hansen and Ottino for a binary abrasive fragmentation, is able to describe an abrasion process generating a manifold of smaller fragments distributed according to a continuous spectrum of fines. The model can be solved in closed form for any fragmentation rate, and for any suitable choice of the distribution of fines.

The fragmentation kernel proposed is not the more general kernel, in that it satisfies the constrain that, at each

breakup event, the same amount of mass is eroded from the mother particle. Thus, the distribution of the mother particles is influenced solely by the critical mass x^* and does not depend upon the number and distribution of fines. However, the formal structure of the model can be applied in a straightforward way to batch fragmentation data, and the value/expression for the parameters/functions entering the model can be easily and accurately recovered from the experimental data. The comparison between model predictions and experimental data available in the literature is satisfactory.

The proposed abrasion model proves a useful tool to investigate the influence of abrasion on dissolution processes. We have addressed the generalization of GAM to include dissolution kinetics. The resulting population balance has been solved in closed form for a kinetically controlled dissolution process. A closed-form solution can be obtained also for more general cases, e.g. in the case the dissolution process is controlled by external transport resistances.

References

[1] C. Varinot, S. Hiltgun, M.-N. Pons, J. Dodds, Chem. Eng. Sci. 52 (1997) 3605.
[2] P.J. Hill, K.M. Ng, AIChE J. 42 (1996) 1600.
[3] H. Berthiaux, C. Varinot, J. Dodds, Chem. Eng. Sci. 51 (1996) 4509.
[4] R.M. Ziff, J. Phys. A: Math. Gen. 24 (1991) 2821.
[5] S. Hansen, J.M. Ottino, Phys. Rev. E 53 (1996) 4209.
[6] S. Hansen, J.M. Ottino, Powder Technol. 93 (1997) 177.
[7] V.S. Vladimirov, Equations of Mathematical Physics, Mir, Moscow, 1984.
[8] W. Tsai, T. Huang, Thin Solid Film 379 (2000) 107.
[9] B.F. Edwards, M. Cai, H. Han, Phys. Rev. A 41 (1990) 5755.
[10] M. Cai, B.F. Edwards, H. Han, Phys. Rev. A 43 (1991) 653.
[11] B. Mazzarotta, Chem. Eng. Sci. 47 (1992) 3105.